Chemistry–A European Journal

Research Article
doi.org/10.1002/chem.202500105

Chemistry
Europe
European Chemical
Societies Publishing

www.chemeurj.org

A Fluorescent Aptasensor for Sensitive and Selective Determination of Epigenetic Cancer Biomarker N¹-Methyladenosine in Urine Samples

Esra Bağda,[a, b] Efkan Bağda,[b, c] and Juewen Liu*[b]

N¹-methyladenosine (m¹A) level in urine increases in the presence of cancer and is associated with the tumor size and stage. In the present study, we aimed to develop a method for rapid, sensitive and accurate determination of m¹A in urine samples. The capture systematic evolution of ligands by exponential enrichment (SELEX) method was used to isolate aptamers that could selectively bind to m¹A. We successfully isolated two sequences that have high selectivity toward m¹A. The affinities against m¹A were determined by isothermal titration calorimetry (ITC) and thioflavin T (ThT) assays. The N1MA1a aptamer has a K_d of 1.9 ± 0.1 μM determined by the ThT assay and 0.75 ± 0.04 μM determined by ITC. A strand-displacement biosensor was designed by labeling the aptamer with a carboxy fluorescein (FAM) and hybridizing it with a quencher-labeled complementary DNA strand. Using this biosensing system, m¹A was detected with a detection limit of 1.9 μM. The system shows high selectivity to m¹A and high tolerance to adenosine, cytidine, guanosine, thymidine, uridine and N⁶-methyladenosine (m⁶A) as well as urine constituents at their real levels in urine. The sensor has been applied to five different human urine samples showing quantitative recovery values, which indicates practical potential of this aptamer-based biosensor.

1. Introduction

In addition to the four fundamental building blocks adenine, uracil, cytosine, and guanine, ribonucleic acid (RNA) also consists of over 150 chemically modified residues. All forms of RNA molecules, including messenger (mRNA), transfer RNA (tRNA), ribosomal (rRNA), and other short and long non-coding RNAs (ncRNAs), have been found to undergo RNA modifications. These modifications are ubiquitous across biological systems, occurring in all kingdoms of life. Numerous of these altered residues are crucial for the synthesis, stability, and dynamics of RNA as well as for RNA splicing, polyadenylation, transport, localization, and translatability. Additionally, they may be crucial for RNA to interact with other molecules, especially those involving proteins and ribonucleoproteins.[1,2] RNA modifications are not static and could be associated with diseases.[3,4]

An adenosine molecule with a methylated N¹ position is known as N¹-methyladenosine (N1MA or m¹A). Among bacterial and eukaryotic RNAs, m¹A methylation is a common and conserved internal post-transcriptional alteration that is mainly present in higher eukaryotic cells. Several investigations have demonstrated the crucial role that m¹A regulates a range of biological processes, including pathogenesis.[5] The translation of the relevant proteins can be inhibited by m¹A in the coding area of mitochondrial transcripts.[6] Due to its disruption of regular Watson-Crick base pairing and increase in local positive charge, m¹A is most likely involved in regulatory processes.[7] In fact, it has been discovered that m¹A reduces the translation of mitochondrial mRNA into protein and is enriched on particular motifs and sections of mRNAs.[3] Increased turnover and RNA degradation, particularly from tRNA, leads to the urinary excretion of methylated nucleosides, which has been observed in higher concentrations in the urine of individuals with various tumor types.[8]

Since modified ribonucleosides are excreted into the urine[9] in different amounts than normal in the presence of some neoplastic diseases, ribonucleoside levels in urine are useful markers for identifying diseases and monitoring treatment response.[10] Modified RNA molecules are metabolized but not reincorporated into tRNA, rather they are excreted into the urine.[9] Zahran et al. emphasized the significant correlation between m¹A with tumor size, stage and nodal status in urine.[11] Besides, Xiong et al. stated that m¹A levels in urine can be measured for early diagnosis of certain diseases as well as for monitoring throughout disease evolution.[5] Urine samples are considered favorable biofluids for the finding of biomarkers due to its noninvasive collection process and simpler matrix than plasma.[12]

The current methods for the determination of adenosine as well as the other nucleosides and their derivatives

[a] E. Bağda
Department of Basic Pharmaceutical Sciences, Analytical Chemistry Division, Faculty of Pharmacy, Sivas Cumhuriyet University, Sivas 58140, Turkiye

[b] E. Bağda, E. Bağda, J. Liu
Department of Chemistry, Waterloo Institute for Nanotechnology, University of Waterloo, Waterloo, ON N2L 3G1, Canada
E-mail: liujw@uwaterloo.ca

[c] E. Bağda
Department of Molecular Biology and Genetics, Faculty of Science, Sivas Cumhuriyet University, Sivas 58140, Turkiye

Chemistry–A European Journal

Research Article
doi.org/10.1002/chem.202500105

Chemistry
Europe
European Chemical
Societies Publishing

in biological fluids require mostly advanced chromatographic techniques.[13–17] In addition, capillary gel electrophoresis combined with solid phase extraction was used for determination of urinary nucleosides and derivatives.[18] These methods require expensive and sophisticated equipment and experts with the skills to apply the methods successfully and meticulously. Besides, various pitfalls connected to mass spectrometry analysis of nucleosides were reported.[19] In addition, they are time-consuming and require laborious pre-processing steps.

Aptamers are single-stranded oligomers that can selectively recognize and bind to their target molecules through electrostatic forces, hydrogen bonding and van der Waals-type intermolecular interactions.[20–23] In certain instances, aptamers transition from an unstructured state to a well-defined tertiary structure upon ligand binding.[24] Aptamers can be chemically synthesized at a low cost. Compared to antibodies, DNA aptamers have fewer batch-to-batch differences, a longer shelf life, and a high tolerance to different molecular milieus and harsh experimental conditions. Besides, they cause lower immunogenicity in vivo.[25,26] Aptamers are isolated with the Systematic Evolution of Ligands by an Exponential Enrichment (SELEX) method.[27,28]

While many aptamers have been selected to bind to adenosine[29,30] as far as we know, no aptamers were developed for m^1A. In m^1A, adenosine is methylated via the N1 position. Due to this structural similarity, selective determination of m^1A is a difficult task. Since in the urine matrix, m^1A coexists with other nucleosides and biomolecules, we aimed to develop a method that is highly selective for m^1A. In this work, we isolated a sequence with the capture-SELEX procedure,[31–33] which showed affinity for m^1A but not for other components. A fluorometric method was developed that allows us to selectively determine m^1A in human urine samples without any sample pretreatment.

2. Experimental Section

2.1. Chemicals

DNA samples were purchased from Integrated DNA Technologies. $MgCl_2 \cdot 6H_2O$, thioflavin T (ThT) and m^1A were purchased from Sigma Aldrich; KCl, $CaCl_2 \cdot 2H_2O$, and NaH_2PO_4 were from Amresco chemicals; NaCl and Tris(hydroxymethyl)aminomethane (Tris) were from VWR BDH chemicals; Na_2SO_4 was from Fisher scientific, m^6A was from Cayman Chemical Company; SSofast EvaGreen Supermix was from BioRad; ThermoPol PCR buffer, dNTP mix and Taq DNA polymerase were from New England Biolabs. 3K and 10K MWCO membrane filters were from Millipore-Sigma (Oakville, ON, Canada). Thermo Scientific Pierce agarose resin was from Fisher Scientific. All buffer solutions were prepared with Milli-Q water ($MQ-H_2O$). The selection buffer contained 50 mM Tris, including 500 mM NaCl and 20 mM $MgCl_2$, pH 7.6. The separation buffer contained 50 mM Tris, including 500 mM NaCl pH 7.6. After adjusting the pH, the buffers were filtered with a 0.2 μm filter.

2.2. SELEX Procedure

For the selection experiments (Figure S1, Supporting Information), the method previously given in the literature was modified and used.[34,35] First, the DNA library containing a 30-nt random region (N30) was annealed with a biotinylated capture strand at 95 °C for 5 min and then allowed to slowly cool to room temperature. A 250 μL of streptavidin-conjugated agarose beads were washed and conditioned with selection buffer. The prepared DNA solution was incubated with the conditioned beads for 20 min and filtered through the beads several times to ensure that the DNA was completely retained, and any remaining DNA was removed by washing the column with selection buffer. A total of 750 μL adenosine (1 mM for negative selection) was loaded into the column, and the DNA portion bound to adenosine was eluted and removed. The column was washed again with the selection buffer. Then, 750 μL m^1A (100 μM) was passed through the column. The eluent was collected, concentrated with a 3K MWCO membrane filter and washed with $MQ-H_2O$. PCR was performed using biotin-reverse primer to amplify the obtained DNA. The PCR product was concentrated with a 10K MWCO membrane filter and washed with separation buffer. DNA was diluted with separation buffer and loaded onto the streptavidin column. After washing the column with separation buffer, ssDNA was eluted with NaOH. The solution was neutralized with HCl, concentrated with a 3K MWCO membrane filter and washed with $MQ-H_2O$. The amount of DNA obtained was determined by a Tecan Spark microplate reader. The amounts of DNA library, adenosine and m^1A used in each cycle of the SELEX procedure are given in Table S1 (Supporting Information).

2.3. DNA Sequencing

The samples were first prepared for PCR with sequencing primers (given in Table S2, Supporting Information). The PCR products were concentrated with 10K MWCO and extracted with small DNA extraction kit (IB scientific). The round 5, 7, 9, 10, 11, 12, and 14 DNA libraries were subjected to deep sequencing. The results were analyzed with Geneious prime software.

2.4. Binding Assays Using ITC

ITC experiments were done with Microcal VP-ITC. A 10 μM DNA and 200 μM target solutions were prepared in SELEX buffer. Samples were degassed prior to the experiment to remove bubbles. A 1.5 mL of DNA sample was loaded into the cell chamber and 280 μL of target molecule was loaded into syringe. The cell temperature was adjusted to 25 °C, reference power was adjusted to 10 μcal/sec, initial delay was adjusted to 180 sec, and stirring speed was adjusted to 351 rpm. The initial injection was 0.5 μL, and subsequent injections were 10 μL. The duration, spacing and filter time were adjusted to 20.0, 360, and 2.0 s, respectively. Origin software was used for fitting the raw data to a one-site binding model. The enthalpy, entropy change, and association constant accompanied to the binding were obtained from the fitted titration curve.

2.5. ThT Fluorescence Based Binding Assays

For ThT fluorescence experiments, a solution with concentrations of 0.7 μM DNA and 16 μM ThT was prepared in selection buffer. The solution was titrated with target solution and the fluorescence intensity was monitored after reaching equilibrium, with a Cary Eclipse fluorescence spectrophotometer. Fluorescence values have been corrected to eliminate the effect of dilution from adding target. The K_d constant was obtained using the nonlinear solution of

Chemistry–A European Journal

Research Article
doi.org/10.1002/chem.202500105

Chemistry
Europe
European Chemical
Societies Publishing

the equation below:

$$F = F_0 - A \frac{[C]}{(K_d + [C])} \tag{1}$$

where F_0 is the initial fluorescence, F is the fluorescence obtained when the target molecule is added, A is the maximum fluorescence decrease, and $[C]$ is the concentration of the target molecule.

2.6. Strand-Displacement Based Fluorescent Biosensing

A s100 pmol of FAM-labeled aptamer was mixed with 200 pmol Iowa Black FQ-labeled quencher DNA in 100 μL of selection buffer and annealed. The solution was slowly cooled to room temperature and stored in the dark. 96 well-plates were used for the experiments and the sensor solution was diluted with selection buffer to provide a final concentration of 20 nM aptamer strand in each well. After the background signal became stable, m^{1}A solution was added to the wells and fluorescence signal recovery was monitored. The Tecan Spark microplate reader was used in the experiments. The excitation wavelength was set to 485 nm, the emission wavelength to 525 nm, and bandwidths to 20 nm. Experiments were performed in triplicate.

2.7. Detection of m^{1}A in Real Urine Samples

The developed sensing method was applied to five different real human urine samples that were collected by lab members. The real human urine (RHU) samples were used without any sample pretreatment steps such as separation or centrifugation. A 2 μL of RHU sample was added to 98 μL sensor solution (with a final aptamer concentration of 20 nM) and the fluorescence signal was recorded after 30 min. The m^{1}A concentration was determined by the calibration graph. Then m^{1}A was spiked into RHU samples and the sensing procedure was applied and the recovery values were calculated. All experiments were performed in 3 replicates.

3. Results and Discussion

3.1. Previous Adenosine Aptamers Cannot Selectively Bind to m^{1}A

Since m^{1}A has an important potential in determining the progression of various cancers,[21] the development of an aptamer for the determination of m^{1}A in complex matrices is the main motivation of this study. m^{1}A differs from adenosine by only one methyl group (Figure 1A). Thus, we first investigated whether the aptamers previously developed for adenosine would bind m^{1}A. For this purpose, we used the Ade1301b, Ade1304b and classical adenosine aptamers (Figure 1B).[29,30] The affinity of these aptamers to m^{1}A and adenosine were determined using the ThT fluorescence assay (Figure 1C). ThT is a DNA staining dye, and it has almost no fluorescence in its free form. The fluorescence intensity of ThT substantially enhances upon binding to DNA. While ThT is best known for binding to G-quadruplex DNA, it can also bind to other DNA structures. Addition of target molecules to the ThT-aptamer system may cause the release of ThT and therefore a fluorescence decrease.[36] This method has

been successfully employed for evaluation the binding of many aptamers.[37–39]

As expected, these aptamers show a high affinity to adenosine, although the Ade1301b aptamer can also bind m^{1}A at about 16-fold lower affinity (Figure 1D). The binding of m^{1}A by the other two aptamers was even weaker and a K_d value cannot be fitted (Figure 1E,F). Therefore, these aptamers are not suitable for the determination of m^{1}A selectively in a complex matrix, where these species may coexist. As a result, an aptamer selective for m^{1}A is needed.

3.2. Selection of Aptamers for m^{1}A

We used the capture SELEX method,[35,34] in which a DNA library with a 30-nucleotide random region (N30) was immobilized onto streptavidin-conjugated beads via hybridization to biotinylated capture strand. The N30 region is flanked by two constant base-pairing regions which can induce folding of the sequence into a hairpin structure. To have high selectivity toward the m^{1}A target, negative SELEX was performed with 1 mM adenosine at the beginning of each round, and the eluted sequences were removed (Table S1, Supporting Information). The concentration of m^{1}A was 100 μM for the first 9 rounds, and it was reduced to 20 μM for the last five rounds. Thus, the adenosine concentration was kept at least 10 times higher than m^{1}A to remove sequences that would also bind adenosine. The sequences obtained by elution with m^{1}A were amplified by PCR. The PCR cycles and progress of the selection were followed using qPCR (Figure S2, Supporting Information). We performed 14 selection rounds and DNA pools from rounds 5, 7, 9, 10, 11, 12, and 14 were sequenced. The N1MA1a and N1MA2a (Figure 2A,B) sequences started to enrich from round 9. N1MA1a, which was found at 2.7% in round 9, had 90% abundance in round 14 (Table S3 and Figure S3, Supporting Information).

3.3. Aptamer Binding Assays

To test if these sequences can bind to m^{1}A, the ThT fluorescence assay was first performed. The results showed that both aptamers can bind to m^{1}A, and the N1MA1a aptamer has a stronger affinity with an apparent K_d of 1.9 μM (Figure 2C). Encouraged by this result, we then tested them using ITC (Figure 2D,E), which also confirmed the affinity of these aptamers to m^{1}A. Again, the affinity of the N1MA1a aptamer (K_d 0.75 μM) was higher affinity than N1MA2a (K_d 7.3 μM) (see Table 1). When m^{1}A was titrated into the Ade1304b aptamer, no binding was detected using ITC (Figure S4 (Supporting Information), confirming the measured m^{1}A aptamer binding was specific. The binding affinity of N1MA1a for m^{1}A is between that of the classical aptamer and the Ade1301b/1304b aptamer for adenosine.[29,30] This is a reasonable result since the N1 site in adenosine is blocked by a methyl group in m^{1}A, and this site can no longer participate in hydrogen bonding. It also suggested that hydrogen bonding of this site might be important for the 1301b/1304b
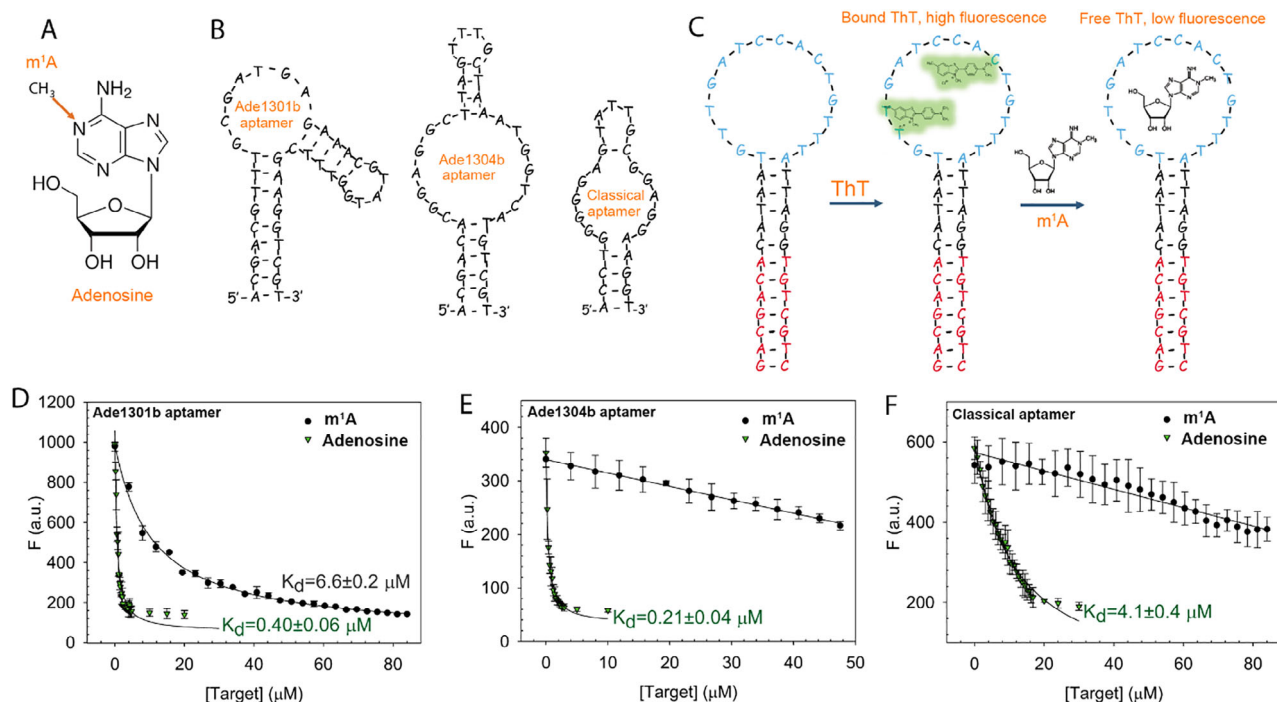
Chemistry–A European Journal

Research Article
doi.org/10.1002/chem.202500105

Chemistry Europe
European Chemical
Societies Publishing

Figure 1. A) The structure of adenosine and the site of methylation to make m^{1}A. B) The secondary structures of the three previously reported DNA aptamers for adenosine. C) The working principle of the ThT replacement assay. The response of the aptamers to adenosine and m^{1}A using the ThT fluorescence assay for D) the Ade1301b aptamer; E) the Ade1304b aptamer; and F) the classical adenosine aptamer. The ThT titrations were performed in the selection buffer.
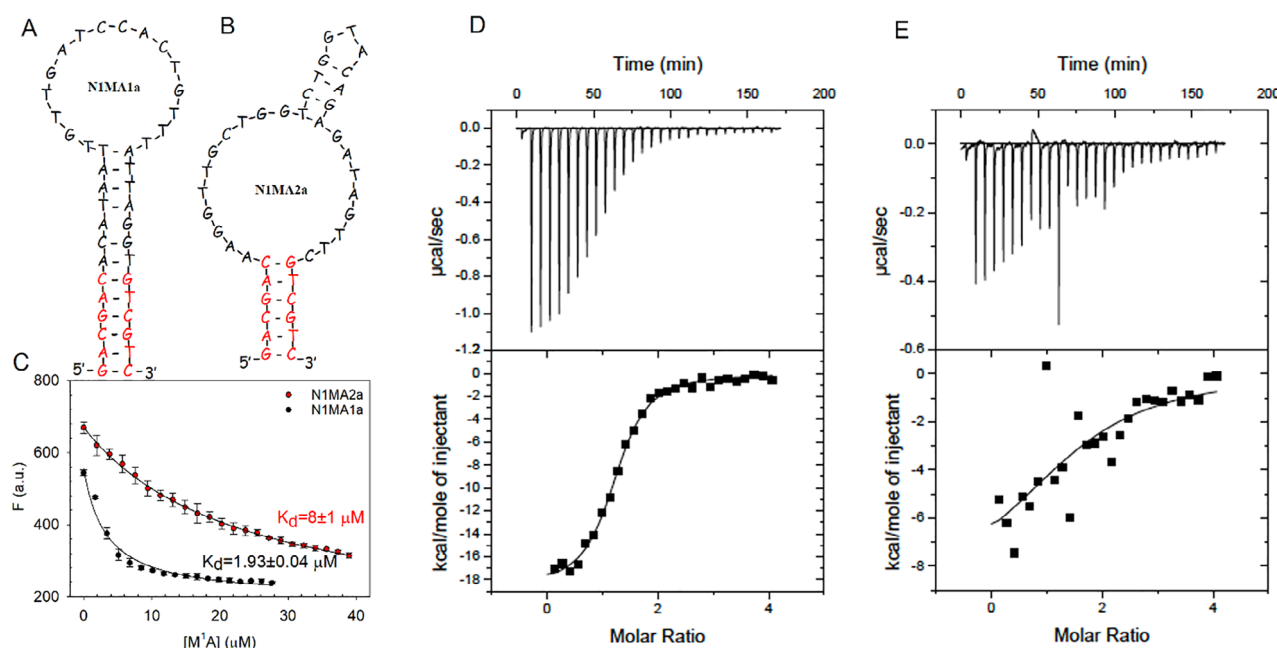

Figure 2. A,B) Secondary structures of the (A) N1MA1a and (B) N1MA2a aptamers. C) ThT fluorescence analysis of aptamer binding. ITC analysis of binding by titrating 200 μM of m^{1}A into D) 10 μM N1MA1a, and E) 10 μM N1MA2a aptamers.

aptamers, which needs to be confirmed by higher-resolution structural biology data. For the N1MA1a aptamer, the binding stoichiometry for m^{1}A is close to 1, suggesting the binding of one target molecule by the aptamer. In addition, the negative enthalpy and negative entropy changes indicated that the binding is enthalpy-driven.

3.4. Sequence Modification Studies

According to the sequence results, the two sequences obtained are N1MA1a and N1MA2a. Since N1MA1a was enriched with a higher percentage, and it has better affinity according to K_d values obtained via ThT assay and ITC, our further studies were

Chemistry–A European Journal

Research Article
doi.org/10.1002/chem.202500105

Chemistry Europe
European Chemical
Societies Publishing

Table 1. The thermodynamic constants obtained from ITC experiments for titration with m^{1}A.

Aptamer	N	K_d [µM]	ΔH [cal/mol][$\times 10^4$]	ΔS [cal/mol/K]
N1MA1a	1.24 ± 0.01	0.75 ± 0.07	−1.86 ± 0.03	−34.4
N1MA2a	1.60 ± 0.6	7.3 ± 7.5	−0.9 ± 0.5	−6.95
N1MA1e	1.0 ± 0.3	8 ± 3	−3 ± 1	−76.6

focused on this aptamer. First, we performed mutation and truncation studies to understand the sequence requirement of this aptamer for target binding (Figure 3A). The N1MA1a aptamer is featured by a stem-loop structure with a very long stem. Modifications were first made in the stem region of the N1MA1a aptamer to make it shorter. For the design of N1MA1b, 7 bases were truncated from the 5′ end of the N1MA1a sequence, while the unmatched A·G base pair was replaced by a A-T pair. For the N1MA1e design, the first six bases in N1MA1a were retained and the subsequent base sequence was truncated up to the loop. For the N1MA1f design, the A·G base pair in the 9th position in N1MA1a was changed to G·A. For N1MA1g, base pairs 8 through 10 in N1MA1a were removed.

ThT assays were performed for all of these truncated sequences, and they all showed similar binding affinities to m^{1}A (Figure 3B). Thus, as long as the stem region is retained, the aptamer can bind to m^{1}A. The ThT assay also conducted for ade-

nine and adenosine. N1MA aptamers showed no affinity to these targets (Figure S5, Supporting Information).

Next, N1MA1c and N1MA1d designs were performed with modifications made in the loop part of N1MA1b. N1MA1c and N1MA1d designs were performed with two modifications that kept the overall secondary structures but with a few conserved nucleotides mutations. In both cases, the ThT assay showed little fluorescence change (Figure 3C). This study confirmed that target binding takes place in this loop region and mutations to the conserved loop nucleotides disrupted aptamer binding. The ITC analysis for N1MA1e to m^{1}A are given in Figure S6 (Supporting Information). The K_d value (K_d 8.1 µM) was similar to that for N1MA2a (Table 1).

3.5. Detection Performance Using a Strand-Displacement Biosensor

Since the N1MA1a aptamer selectively interacts with m^{1}A and has a low K_d value, we planned to develop a sensor with this sequence using the strand displacement method.[40] For this purpose, the 5′ end of the N1MA1a sequence was labeled with a FAM fluorophore (Figure 4A). To make a biosensor, this strand was first hybridized with a quencher-labeled 12-mer DNA (Q-DNA). However, the fluorescence signal of FAM-N1MA1a was not quenched effectively by Q-DNA (Figure 4B). As can be seen from Figure 4A, the long tail part of the N1MA1a sequence provided high
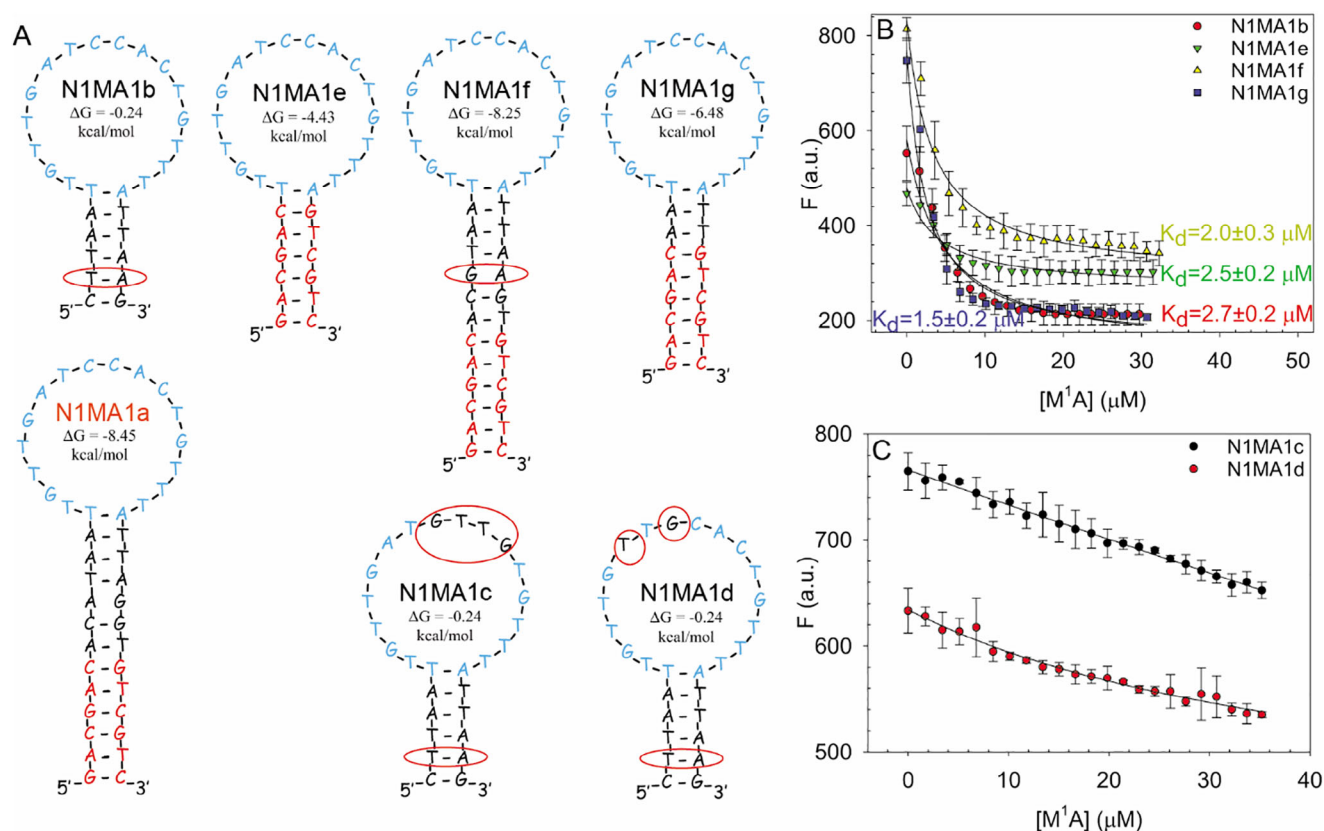

Figure 3. A) The secondary structures of N1MA1 aptamers (the structures and ΔG values were predicted by mFold; [Na$^+$] = 500 mM, [Mg^{2+}] = 20 mM). ThT fluorescence titration curves for m^{1}A into the aptamers: B) N1MA1b, e, f and g, C) N1MA1c and d. The titrations were performed in selection buffer.

Chemistry–A European Journal

Research Article
doi.org/10.1002/chem.202500105

Chemistry Europe
European Chemical
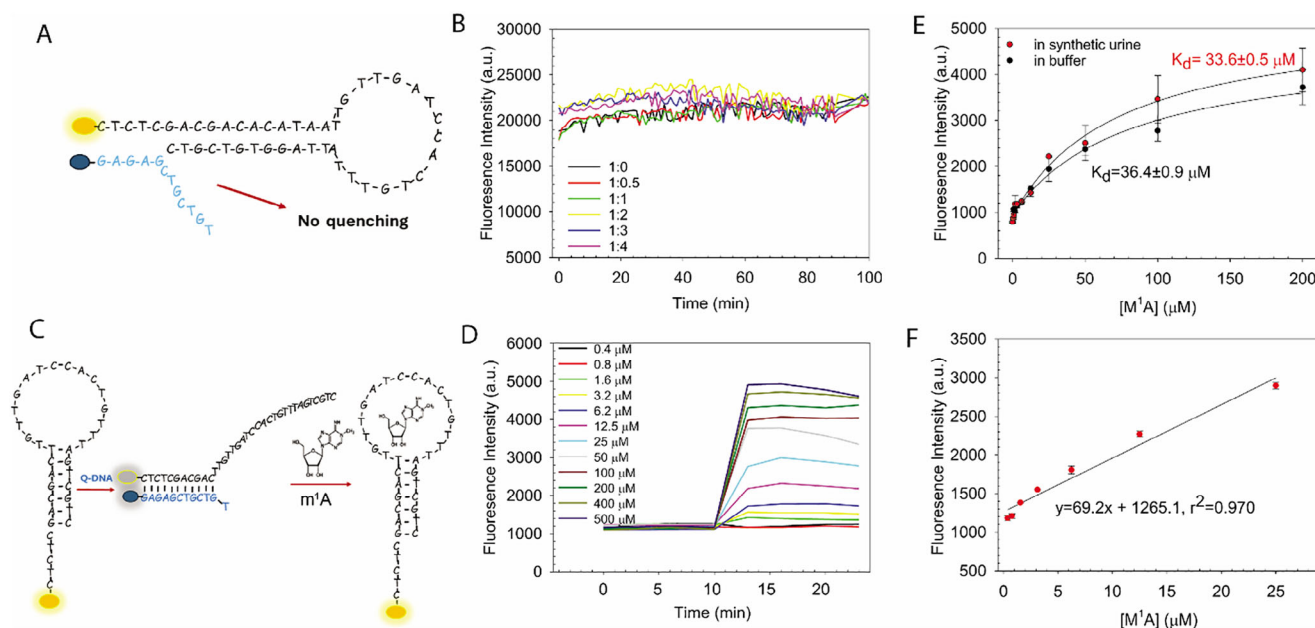Societies Publishing

Figure 4. Aptamer-based fluorescent sensor studies for the detection of m¹A. A) Hybridization of FAM-N1MA1a to the 12-mer Q-DNA failed attributable to the length stem. B) Quenching studies for FAM-N1MA1a at different molar ratios (FAM-N1MA1a: Q-DNA). C) FAM-N1MA1e-based biosensor. D) Kinetic curve for FAM-N1MA1e biosensor system. The target m¹A was added at various concentrations at 10 min. E) Full calibration curves of the sensor in the selection buffer and in synthetic urine for FAM-N1MA1e. F) Linear fluorescence intensity increases as a function of m¹A concentration in the selection buffer for FAM-N1MA1e.

stability and prevented base pairing with Q-DNA. The ΔG value of N1MA1a predicted by mFold was -8.45 kcal/mol (Figure 3A).

Based on these observations, the N1MA1e sequence with a shorter stem sequence (based on the N1MA1e mutant studied above) was labeled with FAM at the 5′ end (FAM- N1MA1e; Figure 4C). The ΔG value of N1MA1e predicted by mFold was only -4.43 kcal/mol, about half of the original sequence (Figure 3A). It was observed that this sequence was effectively quenched by Q-DNA. The background of the sensor was monitored for 10 min, and it was stable (Figure 4D). When m¹A was added, the fluorescence signal increased immediately and remained stable. The fluorescence intensity increased linearly with increasing the m¹A concentration (Figure 4E,F).

A linear calibration was obtained in the concentration range of 0–25 µM m¹A. The analytical sensitivity value was found to be 69.2 fluorescence units µM^{-1}. The detection limit value was found to be 1.9 µM from the 3 sd/m value, where sd is the standard devi-

ation of the blank samples and m is the slope of the calibration curve (Figure 4F).

The selectivity tests were performed with adenosine, cytidine, guanosine, thymidine, uridine and m⁶A, which are structurally similar to m¹A (Figure 5A). The fluorescence recovery obtained for m¹A is much higher compared to the other molecules and is quite significant for all three concentrations. Some fluorescence increase was observed for 200 µM concentration levels, but the recovery ranges were quite weak compared to m¹A. This confirms the selectivity of the aptamer for m¹A.

3.6. Measurement of m¹A in Synthetic Urine

Since the sensor developed for the determination of m¹A in urine, the sensor responses of the ions and constituents found in urine were tested separately. As shown in Figure 5B, none
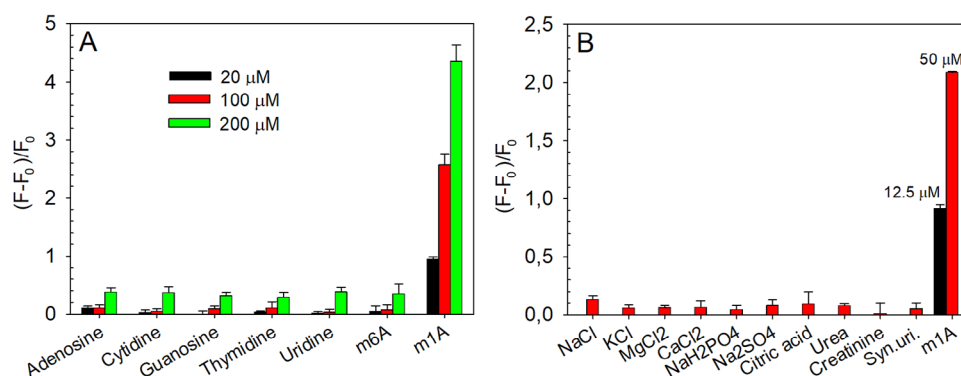

Figure 5. A) Selectivity test for FAM-N1MA1e biosensing system with similar biomolecules. B) Selectivity test for FAM-MA1e biosensing system to urine matrix constitutes. The concentrations of urine components are in Table S4 (Supporting Information).

Chem. Eur. J. **2025**, *31*, e202500105 (6 of 8)

© 2025 The Author(s). Chemistry – A European Journal published by Wiley-VCH GmbH

Chemistry–A European Journal

Research Article
doi.org/10.1002/chem.202500105

Chemistry Europe
European Chemical
Societies Publishing

of the ions or molecules in the formulation of synthetic urine induced a sensor response. In addition, a synthetic urine sample with all the components together was tested (synthetic urine bar in Figure 5B). It was found that the system tolerated the matrix constituents well (Figure 5B). Urine components increase the fluorescence signal, albeit relatively slightly. The reason for the slight fluorescence signal differences seen in Figure 4E is attributed to the high ion concentration of the synthetic urine matrix. We also titrated m^1A in synthetic urine, and the apparent K_d value was 33.6 μM, which was close to the K_d of 36.4 μM in clean buffer (Figure 4E). The K_d value is much higher than what was measured with ITC and ThT. The reason for this is that there is competition in the strand displacement method.[40] All of these studies prove that the developed sensor system has a very high tolerance to both similar molecules and urine components, thus proving that this system has a very excellent selectivity for m^1A.

3.7. Determination of m^1A in Real Urine Samples

Finally, the developed method was applied to a real human urine sample (RHU) determine the m^1A concentration. While applying the method, RHU samples were used raw without any sample pretreatment such as separation or centrifugation. The RHU samples were diluted 50-fold into buffer containing the sensor for measurement. In addition, spiked RHU samples were tested after determining the m^1A concentration in the raw RHU samples. The m^1A concentrations (before and after spiking) of RHU and spiked RHU samples are given in Table S5 (Supporting Information). Percentage recovery values are in the range of 86–116%. These data confirm that the developed method was successfully applied to complex real human urine samples where m^1A is present.

4. Conclusion

In this study, we developed a method for the determination of m^1A in urine samples. Since the urine matrix is complex and there may be biomolecules with similar structures to m^1A in urine, the method needed to be selective for m^1A. The N1MA1a and N1MA2a aptamers were successfully isolated with the capture SELEX method. In the method, negative SELEX was performed in all steps so that similar compounds would not show affinity to the isolated aptamers. The affinities of these sequences were confirmed with ThT assays and ITC. N1MA1a showed with high selectivity and affinity for m^1A. From the mutant sequences obtained by modifications made to this isolated sequence, a biosensor system that showed selectivity for the determination of m^1A in urine matrix, and that has high tolerance to urine components and similar biomolecules was successfully developed. The developed fluorescence system was successfully applied to determine m^1A with high accuracy in a complex urine matrix without laborious separation processes.

Conflict of Interests

The authors declare no conflict of interests.

Data Availability Statement

The data that support the findings of this study are available from the corresponding author upon reasonable request.

[1] W. Dai, N. J. Yu, R. E. Kleiner, *Acc. Chem. Res.* **2023**, *56*, 2726.

[2] J. Mo, X. Weng, X. Zhou, *Acc. Chem. Res.* **2023**, *56*, 2788.

[3] Z. Su, I. Monshaugen, B. Wilson, F. Wang, A. Klungland, R. Ougland, A. Dutta, *Nat. Commun.* **2022**, *13*, 2165.

[4] B. Chen, B.-F. Yuan, Y.-Q. Feng, *Anal. Chem.* **2019**, *91*, 743.

[5] W. Xiong, Y. Zhao, Z. Wei, C. Li, R. Zhao, J. Ge, B. Shi, *Mol. Ther.* **2023**, *31*, 308.

[6] C. Zhang, G. Jia, *Genom. Proteom. Bioinform.* **2018**, *16*, 155.

[7] J. Smoczynski, M.-J. Yared, V. Meynier, P. Barraud, C. Tisné, *Acc. Chem. Res.* **2024**, *57*, 429.

[8] A. Seidel, S. Brunner, P. Seidel, G. I. Fritz, O. Herbarth, *Br. J. Cancer* **2006**, *94*, 1726.

[9] L. Zhang, W. Zhang, H. Wang, *Anal. Chem.* **2024**, *96*, 11366.

[10] T. Niwa, N. Takeda, H. Yoshizumi, *Kidney Int.* **1998**, *53*, 1801.

[11] F. Zahran, R. Rashed, M. Omran, H. Darwish, A. Belal, *Indian J. Clin. Biochem.* **2021**, *36*, 319.

[12] X. Zhang, Y. Hu, X. Hong, M. Wang, Z. Fang, X. Cao, K. Jiang, C. Guo, *J. Chromatogr. B* **2022**, *1209*, 123428.

[13] Y. Xie, K. A. Janssen, A. Scacchetti, E. G. Porter, Z. Lin, R. Bonasio, B. A. Garcia, *Anal. Chem.* **2022**, *94*, 7246.

[14] E. Dudley, F. Lemiere, W. V. Dongen, J. I. Langridge, S. El-Sharkawi, D. E. Games, E. L. Esmans, R. P. Newton, *Rapid Commun. Mass Spectrom.* **2001**, *15*, 1701.

[15] H. Li, S. Wang, H. Liu, S. Bu, J. Li, D. Han, M. Zhang, G. Wu, *J. Mass Spectrom.* **2009**, *44*, 641.

[16] H. Zhang, L. Liu, M. Li, *ACS Sens.* **2024**, *9*, 1089.

[17] M. Zhang, Y. Xiao, Z. Jiang, C. Yi, *Acc. Chem. Res.* **2023**, *56*, 2980.

[18] E. Szymańska, M. J. Markuszewski, M. Bodzioch, R. Kaliszan, *J. Pharm. Biomed. Anal.* **2007**, *44*, 1118.

[19] G. Ammann, M. Berg, J. F. Dalwigk, S. M. Kaiser, *Acc. Chem. Res.* **2023**, *56*, 3121.

[20] M. R. Dunn, R. M. Jimenez, J. C. Chaput, *Nat. Rev. Chem.* **2017**, *1*, 0076.

[21] Y. Wu, L. Li, L. Wang, S. Zhang, Z. Zeng, J. Lu, Z. Wang, Y. Zhang, S. Zhang, H. Li, T. Chen, *BMC Cancer* **2024**, *24*, 506.

[22] H. Yu, O. Alkhamis, J. Canoura, Y. Liu, Y. Xiao, *Angew. Chem., Int. Ed.* **2021**, *60*, 16800.

[23] S. Qian, D. Chang, S. He, Y. Li, *Anal. Chim. Acta* **2022**, *1196*, 339511.

[24] M. Domsicova, J. Korcekova, A. Poturnayova, A. Breier, *Int. J. Mol. Sci.* **2024**, *25*, 6833.

[25] X. Wu, Y. Liu, D. Zhang, J. Yu, M. Zhang, S. Feng, L. Zhang, T. Fu, Y. Tan, T. Bing, W. Tan, *J. Am. Chem. Soc.* **2024**, *146*, 26667.

[26] D. J. Chinchilla-Cárdenas, J. S. Cruz-Méndez, J. M. Petano-Duque, R. O. García, L. R. Castro, M. J. Lobo-Castañón, G. O. Cancino-Escalante, *J. Genet. Eng. Biotechnol.* **2024**, *22*, 100400.

[27] Y. Ding, J. Liu, *Anal. Chem.* **2023**, *95*, 14651.

[28] X. Wang, W. Xie, H. Peng, *Environ. Health* **2023**, *1*, 72.

[29] D. E. Huizenga, J. W. Szostak, *Biochemistry* **1995**, *34*, 656.

[30] Y. Ding, J. Liu, *J. Am. Chem. Soc.* **2023**, *145*, 7540.

[31] S. Y. Lam, H. L. Lau, C. K. Kwok, *Biosensors* **2022**, *12*, 1142.

[32] Y. Zhang, S. Zhang, Z. Ning, X. Lin, N. Duan, Z. Wang, S. Wu, *J. Agric. Food Chem.* **2024**, *72*, 28148.

[33] G. H. Lee, Y. Kim, E. S. Lee, D. Nam, B. S. Cha, S. Kim, S. Kim, K. S. Park, *BioChip J.* **2024**, *18*, 601.

[34] K.-A. Yang, R. Pei, M. N. Stojanovic, *Methods* **2016**, *106*, 58.

[35] P.-J. J. Huang, J. Liu, *Anal. Chem.* **2022**, *94*, 3142.

[36] F. Y. Khusbu, X. Zhou, H. Chen, C. Ma, K. Wang, *TrAC Trends Anal. Chem.* **2018**, *109*, 1.

[37] Y. Ding, Y. Xie, A. Z. Li, P.-J. J. Huang, J. Liu, *Biochemistry* **2023**, *62*, 2280.

[38] S. Stangherlin, Y. Ding, J. Liu, *Small Methods* **2024**, 2401572.

[39] K. Yang, N. M. Mitchell, S. Banerjee, Z. Cheng, S. Taylor, A. M. Kostic, I. Wong, S. Sajjath, Y. Zhang, J. Stevens, S. Mohan, D. W. Landry, T. S. Worgall, A. M. Andrews, M. N. Stojanovic, *Science* **2023**, *380*, 942.

[40] R. Nutiu, Y. Li, *J. Am. Chem. Soc.* **2003**, *125*, 4771.